Cancer Research

miR-9 and miR-200 Regulate PDGFRβ-Mediated Endothelial Differentiation of Tumor Cells in Triple-Negative Breast Cancer

Elvira D'Ippolito[1], Ilaria Plantamura[1], Lucia Bongiovanni[2], Patrizia Casalini[3], Sara Baroni[1], Claudia Piovan[1], Rosaria Orlandi[3], Ambra V. Gualeni[4], Annunziata Gloghini[4], Anna Rossini[5], Sara Cresta[5], Anna Tessari[5], Filippo De Braud[5,6], Gianpiero Di Leva[7], Claudio Tripodo[2], and Marilena V. Iorio[1]

Abstract

Organization of cancer cells into endothelial-like cell-lined structures to support neovascularization and to fuel solid tumors is a hallmark of progression and poor outcome. In triple-negative breast cancer (TNBC), PDGFRβ has been identified as a key player of this process and is considered a promising target for breast cancer therapy. Thus, we aimed at investigating the role of miRNAs as a therapeutic approach to inhibit PDGFRβ-mediated vasculogenic properties of TNBC, focusing on miR-9 and miR-200. In MDA-MB-231 and MDA-MB-157 TNBC cell lines, miR-9 and miR-200 promoted and inhibited, respectively, the formation of vascular-like structures *in vitro*. Induction of endogenous miR-9 expression, upon ligand-dependent stimulation of PDGFRβ signaling, promoted significant vascular sprouting of TNBC cells, in part, by direct repression of STARD13. Conversely, ectopic expression of miR-200 inhibited this sprouting by indirectly reducing the protein levels of PDGFRβ through the direct suppression of ZEB1. Notably, *in vivo* miR-9 inhibition or miR-200c restoration, through either the generation of MDA-MB-231–stable clones or peritumoral delivery in MDA-MB-231 xenografted mice, strongly decreased the number of vascular lacunae. Finally, IHC and immunofluorescence analyses in TNBC specimens indicated that PDGFRβ expression marked tumor cells engaged in vascular lacunae. In conclusion, our results demonstrate that miR-9 and miR-200 play opposite roles in the regulation of the vasculogenic ability of TNBC, acting as facilitator and suppressor of PDGFRβ, respectively. Moreover, our data support the possibility to therapeutically exploit miR-9 and miR-200 to inhibit the process of vascular lacunae formation in TNBC. *Cancer Res; 76(18); 5562–72. ©2016 AACR.*

Introduction

Tumor vascularization is a fundamental step in solid tumor progression. The idea that this process only relies on the sprouting of existing endothelial angiogenic vessels has been gradually replaced by the evidence that tumor vasculature is orchestrated by different pathways of vasculogenesis. Indeed, the contribution of neoplastic cells is increasingly relevant (1). More importantly, the presence of noncanonical mechanisms of tumor-mediated vascularization (e.g., vascular mimicry, tumor to endothelial-like cell differentiation, vessel co-option) is particular to more aggressive cancers and has been associated with tumor progression and decreased survival rate (1).

The differentiation of tumor cells in endothelial-like cells was reported in angiogenic vessels of aggressive cancers, where neoplastic cells acquired the expression of endothelial markers (e.g., CD31 and CD34) and participated in the formation of functional vascular-like structures (2, 3). We recently described the presence of vascular lacunae lined by a mosaic of normal endothelial cells and CD31-expressing tumor cells in human breast cancer (4). Among the different breast cancer subtypes, we reported that the endothelial differentiation ability was most prominent in triple-negative breast cancer (TNBC), the most aggressive and undifferentiated subtype (5, 6), where the presence of vascular lacunae associated with poor clinical outcome. Moreover, treatment with multi-target tyrosine kinase inhibitors (TKI) reduced the formation of these structures, nominating platelet-derived growth factor receptor beta (PDGFRβ) as an important player in this alternative mechanism of vascularization (4). Interestingly, PDGFR signaling has been under investigation as a promising target for breast cancer therapy due to its involvement in crucial steps of progression such as angiogenesis, epithelial-to-mesenchymal

[1]Start Up Unit, Department of Experimental Oncology and Molecular Medicine, Fondazione IRCCS Istituto Nazionale dei Tumori, Milan, Italy. [2]Tumor Immunology Unit, Department of Health Sciences, University of Palermo, Palermo, Italy. [3]Molecular Targeting Unit, Department of Experimental Oncology and Molecular Medicine, Fondazione IRCCS Istituto Nazionale dei Tumori, Milan, Italy. [4]Department of Diagnostic Pathology and Laboratory Medicine, Fondazione IRCCS Istituto Nazionale dei Tumori, Milan, Italy. [5]Department of Medical Oncology, Fondazione IRCCS Istituto Nazionale dei Tumori, Milan, Italy. [6]Department of Oncology and Hematology-Oncology, University of Milan, Milan, Italy. [7]Environment & Life Sciences, University of Salford, Salford, United Kingdom.

Note: Supplementary data for this article are available at Cancer Research Online (http://cancerres.aacrjournals.org/).

E. D'Ippolito and I. Plantamura contributed equally to this article.

Corresponding Author: Marilena V. Iorio, Start Up Unit, Department of Experimental Oncology and Molecular Medicine, Fondazione IRCCS Istituto Nazionale dei Tumori, Via Amadeo 42, Milan 20133, Italy. Phone: 3902-2390-5134/26; Fax: 3902-2390-2692; E-mail: marilena.iorio@istitutotumori.mi.it

doi: 10.1158/0008-5472.CAN-16-0140

transition (EMT), and metastasis (7). However, clinical trials with TKIs against this receptor have not produced satisfactory results (7).

miRNAs are small noncoding RNA molecules involved in gene regulation that are often deregulated in human cancer (8). Interestingly, a negative regulatory loop involving miR-9 and PDGFRβ has been described in a cardiomyocyte model (9). In this context, ligand-dependent stimulation of PDGFRβ triggers activation of the downstream signaling pathways. PDGFRβ signaling induces the expression of miR-9, which acts to inhibit PDGFRβ activation by targeting the mRNA encoding this receptor. Together with the internalization and degradation of PDGFRβ upon stimulation, this provides a mechanism by which signaling through this receptor may be temporally limited. High levels of miR-9 have been associated with prometastatic function in human breast cancer (10), as well as with the acquisition of a mesenchymal and aggressive phenotype (11). On the other hand, members of the miR-200 family (five miRNAs organized in two clusters: miR-200a/b/429 and miR-200c/141) are well-known negative regulators of EMT due to their direct targeting of several transcriptional factors implicated in the transition, such as ZEB1/2 and Snail (12). Interestingly the EMT-associated transcriptional factors FOXQ1 and TWIST1 can induce PDGFR expression (13). Conversely, PDGFRβ activation with PDGF-DD ligand mediates EMT through the induction of ZEB1 and consequent suppression of miR-200 (14).

Here, we investigated the role of miR-9 and miR-200 in the PDGFRβ-mediated vasculogenic properties of TNBC, raising the possibility of a new miRNA-based therapeutic approach to impair the phenomenon of vasculogenesis in TNBC.

Materials and Methods

Patients and samples

Human tissues were selected from the archives of the Fondazione IRCCS Istituto Nazionale dei Tumori of Milan (INT) from patients with invasive breast cancer and naïve of neoadjuvant treatment. The first set included 78 formalin-fixed paraffin embedded (FFPE) breast cancers collected from 2003 to 2004 (29 luminal, 32 $HER2^+$, and 17 TNBCs). The second set consisted of 85 FFPE TNBC, resected between 2002 and 2006 (baseline characteristics of the two cohorts in Supplementary Table S1). Histologic subtype and grade were determined according to WHO classification and Nottingham histologic grading system, respectively. Immunohistochemical classification was assigned following the 2009 St. Gallen's Consensus guidelines for estrogen receptor (ER) and progesterone receptor (PgR) markers, whereas HER2 was scored according to ASCO/CAP 2013 guidelines. An informed consent was obtained from all patients. All procedures were carried out in accordance with the Helsinki Declaration (World Medical Association, 2013) and the study was conducted only after approval from the Institutional Review Board and the Independent Ethical Committee.

Cell cultures, plasmids, and treatments

Human TNBC cell lines MDA-MB-231, MDA-MB-157, MDA-MB-468, and HCC1937, and embryonic kidney HEK293 cells were purchased from ATCC. SUM149 and SUM159 TNBC cell lines were purchased from Asterand Bioscience. All cell lines were obtained between 2000 and 2010, authenticated once a year (last verification on November 2015) using the short tandem repeat profiling method in our Institute facility, and propagated in the suggested media within 6 months of thawing from stocks.

Clones stably expressing miR-9 inhibitor and miR-200c precursor were generated from the MDA-MB-231 cell line after transfection with pEZX-AM01 and pEZX-AM04 plasmids (GeneCopoeia), respectively, using Lipofectamine 3000 transfection reagent (Life Technologies). Cells were cultured in RPMI1610 medium with 10 % FBS, 1 mmol/L L-glutamine, and 0.75 μg/mL (miR-9 clones) or 0.5 μg/mL (miR-200c clones) puromycin.

For PDGFRβ stimulation, cells were treated with 50 ng/mL PDGF-BB (Peprotech) in serum-free medium and maintained in serum-free medium.

miRNA and siRNA transfection

miRNA overexpression was achieved by transfection with human miRNA precursors (Life Technologies) and verified by qRT-PCR. miRNA silencing was obtained by transfection with locked nucleic acid (LNA)-based inhibitors (Exiqon) and validated by reporter assay. For gene knockdown, specific siRNAs (Life Technologies) were used. Cells were incubated with 100 nmol/L miRNA precursors, LNAs, or siRNAs complexed with Lipofectamine RNAi Max transfection reagent (Life Technologies) according to manufacturer's instructions.

RNA extraction and quantitative RT-PCR

Total RNA was extracted from cell lines with QIAzol reagent (Qiagen). For gene and miRNA quantification, cDNA was synthesized from 1 μg and 100 ng of RNA with SuperScript III Reverse Transcriptase and TaqMan MiRNA Reverse Trascription Kit (Life Technologies), respectively. qRT-PCR was performed using TaqMan assays for human *ZEB1*, *GAPDH*, miR-9-5p, miR-200b-3p, miR-200c-3p, and *RNU44* (Life Technologies) or custom primers for *PDGFRβ* and *GAPDH* with SYBR Green technology (Life Technologies). From FFPE breast cancer tissues, total RNA was extracted with miRNeasy Mini Kit (Qiagen) and assessed for quality via Bioanalyzer. Twenty nanograms of RNA were reverse transcribed using miRCURY LNA Universal RT miRNA PCR system (Exiqon) and qRT-PCR was performed in triplicate using Exiqon assays for human miR-9-5p, miR-200c-3p, *RNU44*, and *RNU48*. Gene and miRNA levels were normalized to the endogenous control *RNU44*, *RNU48*, or *GAPDH* and the relative expression was calculated using the comparative $2^{-\Delta C_t}$ method.

Primers: *GAPDH* Fw: 5′-ATTCCACCCATGGCAAATTC-3′; *GAPDH* Rv: 5′-AGCATCGCCCCACTTGATT-3′; *PDGFRβ* Fw: 5′-AGCGCTGGCGAAATCG-3′; *PDGFRβ* Rv: 5′-TGACACTGGTTCGCGTGAA-3′.

Western blot analysis

Total protein lysates were extracted with lysis buffer (1% Triton, 50 nmol/L Tris, 15 mmol/L NaCl) supplemented with protease inhibitors (Sigma-Aldrich). The following primary antibodies were used: rabbit anti-human IgG antibodies against STARD13 (1:500, sc-67843), PDGFRβ (1:500, sc-432), E-cadherin (1:500, sc7870; Santa Cruz Biotechnology); mouse anti-human IgG antibody against Vinculin (1:1,000, V9131, Sigma-Aldrich); mouse horseradish peroxidase–conjugated anti-human IgG anti-β-actin (1:1,000, A3854, Sigma-Aldrich). Proteins were visualized by enhanced chemiluminescence detection system (Sigma-Aldrich). Quantification was performed by Quantity One 4.6.6 software (Bio-Rad).

Reporter assay

Cells (8×10^4) were seeded in 24-well plates and cotransfected with 500 ng pMiR-9-5p-Luc reporter vector (Signosis) and 50 ng phRL-SV40 control vector (*Renilla*; Promega) using Lipofectamine 3000. After 24 hours, Firefly and *Renilla* luciferase activities were measured by Dual-Luciferase Reporter Assay System (Promega).

Tube formation assay

Plates (96-well) were coated with growth factor–reduced Matrigel (Corning) and tube formation assay was performed and quantified as reported previously (4).

Dual-luciferase reporter assay

The full-length human 3′UTR of STARD13 was cloned in pmirGLO Dual-Luciferase miRNA Target Expression vector (Promega; pmiR-3′UTRWT). This construct was used to generate plasmids carrying the mutated forms of STARD13 3′UTR, modified in each of the two predicted miR-9–binding sites (pmiR-3′UTRMut1 and pmiR-3′UTRMut2), using QuikChange II XL Site-Directed Mutagenesis Kit (Agilent). HEK293 cells (2×10^5) were seeded in 12-well plates and cotransfected with 500 ng pmiR-3′UTR (WT, Mut1, or Mut2) and 100 nmol/L of either miR-9-5p precursor or negative control using Lipofectamine 3000. After 24 hours, Firefly and *Renilla* luciferase activities were measured as described above.

***In silico* analyses**

Level 3 TCGA data from mRNA-seq and miR-seq of breast cancer samples were used. To define tumor subtype, we used ER, PgR, and HER2 IHC status reported in the clinical information file.

Profiling data of 175 nitrogen-frozen breast cancer tissues had been deposited by Huang and colleagues in the Gene Expression Omnibus data repository (GEO) with accession number GSE59590 (15). For the Italian subset, differentially expressed genes between luminal and basal breast cancers were identified by linear modeling as implemented in the limma package (16). *In silico* prediction of miRNA targets was performed with 6 algorithms simultaneously (DIANAMicroT-CDS, miRanda, miRDB, PITA, RNA22, TargetScan v6.2; ref. 17) using the HUGO gene symbol as common identifier.

***In vivo* experiments**

Orthotopic breast tumors were generated by implantation of 5×10^6 cells resuspended in a 1:1 mixture of PBS and Matrigel (Corning) in the mammary fat pad of 8-week-old female SCID mice (Charles Rivers). For stable clones, tumors were monitored and harvested before necrosis. For *in vivo* miRNA modulation, when MDA-MB-231 tumors reached a volume of approximately 50 mm^3, mice were treated with 20 μg miRNA-based drugs (Tema Ricerca) administered five times, every 3–4 days, by peritumoral injection. miR-9 inhibitor or control were delivered as naked oligonucleotides, whereas miR-200c mimic or cel-miR-67 control were formulated with MaxSuppressor In Vivo RNA-LANCEr II (Bioo Scientific), according to manufacturer's instructions. All animal experiments were approved by the Ethics Committee for Animal Experimentation of INT.

Immunohistochemical analysis

FFPE xenograft tumor sections were unmasked using Novocastra Epitope Retrieval Solutions pH 6 and pH 9 and incubated for 1 hour with the following primary antibodies at room temperature: mouse anti-human CD31 (1:50, 1A10, Leica Biosystems); mouse anti-human AREB6 (ZEB1; 1:150, 3G6, Abcam).

FFPE human specimens were treated with citrate solution to unmask the antigen and then incubated for 1 hour with rabbit anti-human PDGFRβ (1:200, Y92, Abcam) at room temperature.

Immunofluorescence

FFPE human sections were incubated with the following primary antibodies: mouse anti-human CD31 (1:50 pH6, 1A10, Leica Biosystems), rabbit anti-human PDGFRβ (1:250 pH6, Y92, Abcam), and mouse anti-human p53 (1:800 pH6, DO-7, Leica Biosystems). The following secondary antibodies were used: Alexa Fluor 350–conjugated goat anti-mouse, Alexa Fluor 488–conjugated goat anti-rabbit, Alexa Fluor 568–conjugated goat anti-mouse (Life Technologies).

miRNA *in situ* hybridization

miRNA *in situ* hybridization (ISH) was performed as described previously (18). Tumor sections were hybridized with double-DIG-LNA probes for miR-21, miR-9, miR-200c, and scrambled miR (Exiqon), according to the manufacturer's instructions.

Statistical analysis

For two-group comparison, multiple group comparison and correlation analyses, the probability value was calculated, respectively, with either an unpaired two-tailed Student *t* test or nonparametric Mann–Whitney test, nonparametric Kruskal–Wallis test, or moderated *t* test adjusted for multiple testing by the false discovery rate (FDR) on limma package in R, and Pearson test using GraphPad Prism 5 software (GraphPad software Inc.). Statistical significance of association analyses and differences in survival Kaplan–Meier curves were tested with χ^2 and Wilcoxon test, respectively, using SAS software (SAS Institute Inc.). $P \leq 0.05$ was considered significant.

Data are expressed as mean ± SD of three independent experiments, unless otherwise specified in the figure legends.

Results

miR-9 mediates PDGFRβ-induced tube formation ability

Among a panel of TNBC cell lines, we selected MDA-MB-231 and MDA-MB-157 as suitable models based on their described ability to generate vascular-like structures *in vitro* (4) and on the opposite expression of miR-9 (Supplementary Fig. S1A). We first confirmed the previously described negative regulatory loop existing between miR-9 and PDGFRβ (9). Specifically, PDGFRβ protein levels were reduced upon overexpression of miR-9 in MDA-MB-231 cells, and increased following inhibition of this miRNA in MDA-MB-157 cells (Supplementary Fig. S1B and S1C), corroborating the targeting of the receptor by miR-9. Further reporting the previously described regulatory relationship between PDGFRβ and miR-9 (9), activation of PDGFRβ with PDGF-BB ligand increased the relative expression of miR-9 in both TNBC models (Fig. 1A).

We thus investigated the functional effect of miR-9 in tube formation capability. MDA-MB-231 cells transfected with miR-9 precursor acquired a higher ability to form vascular-like structures than control cells, whereas silencing of miR-9 in MDA-MB-157 cells resulted in a strong impairment of the same phenomenon (Fig. 1B). These data suggest that miR-9 could contribute to

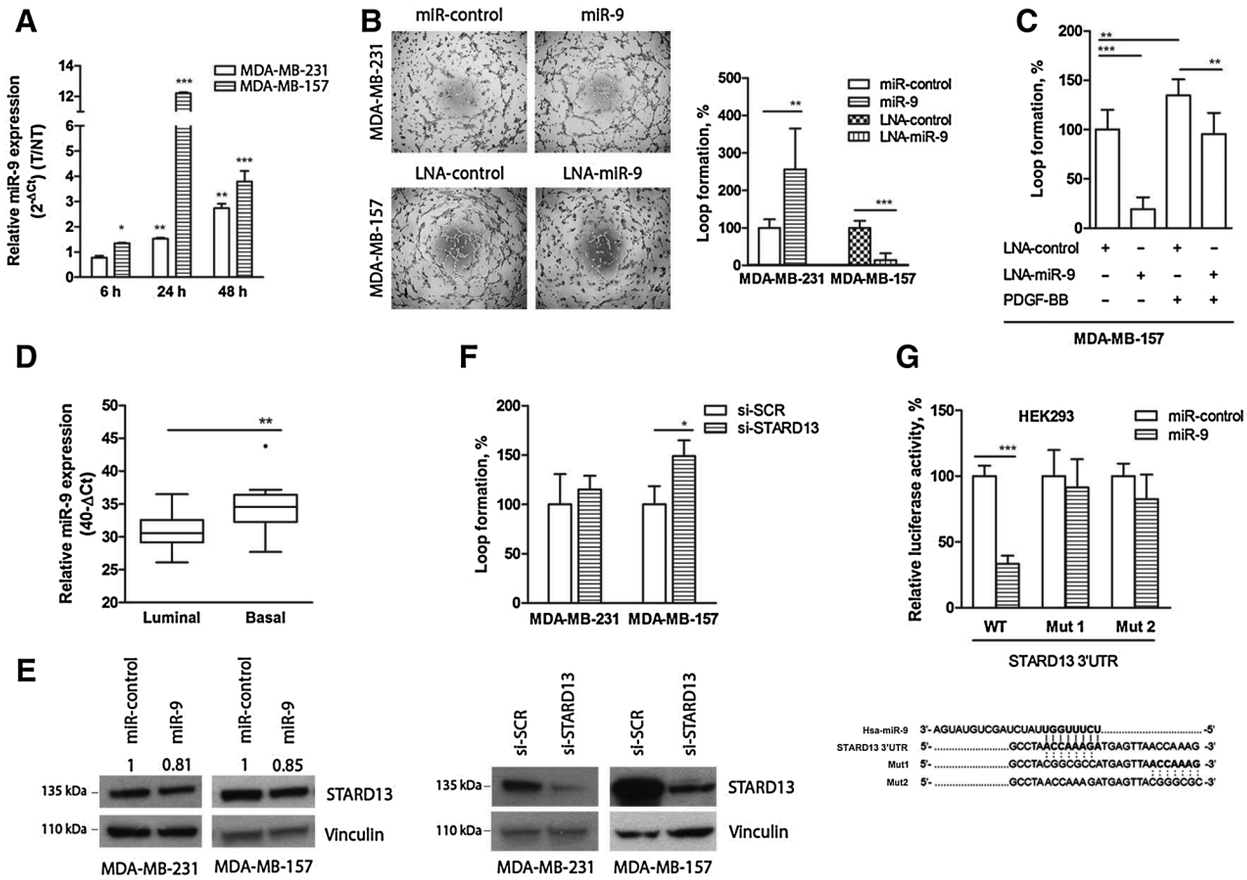

Figure 1.

miR-9 mediates PDGFRβ-induced tube formation ability through STARD13 targeting. **A,** TNBC cells were treated with 50 ng/mL PDGF-BB for 6 hours. miR-9 expression was assessed by qRT-PCR. The result is representative of three independent experiments and is expressed as mean ± SD of three technical replicates. **B,** TNBC cells were transfected with either miR-9 precursor or LNA-miR-9, and corresponding controls, for 48 hours; tube formation ability was determined as the percentage of modulation in loop formation of treated cells compared with control. **C,** MDA-MB-157 cells were transfected with either LNA-miR-9 or LNA-control and, after 24 hours, treated or not with PDGF-BB for the following 24 hours; tube formation ability was evaluated. **D,** miR-9 expression in basal versus luminal breast cancer was evaluated by qRT-PCR; statistically significant differences were calculated with Mann–Whitney test. **E,** TNBC cells were transfected with either miR-9 precursor or control for 48 hours. STARD13 protein was evaluated by Western blot analysis. **F,** TNBC cells were transfected with a siRNA specific against STARD13 or a scrambled oligonucleotide for 48 hours; tube formation assay was performed (top). Efficiency of silencing was validated by Western blot analysis (bottom). **G,** HEK293 cells were cotransfected with either control or miR-9 precursor and with pmiR-Glo dual-luciferase reporter plasmid carrying the wild-type (WT) or the mutated forms (Mut1 and Mut2) of STARD13 3′UTR. Firefly luciferase activity was measured 24 hours after transfection, normalized on *Renilla* luciferase, and expressed as relative value between cells transfected with miR-9 and the corresponding control. *, $P < 0.05$; **, $P < 0.01$; ***, $P < 0.001$, Student *t* test.

PDGFRβ-regulated vasculogenesis. To strengthen these findings, MDA-MB-157 cells were transfected with either LNA-miR-9 or a scrambled oligonucleotide, and PDGF-BB–treated cells were compared with control cells. We observed that the advantage in loop formation ability gained with the treatment with PDGF-BB was almost completely abrogated by concomitant knockdown of miR-9 (Fig. 1C).

In summary, miR-9 enhances the ability of TNBC cells to generate vascular-like structures in response to PDGFRβ *in vitro*.

miR-9 is overexpressed in TNBC and associates with poor prognosis in breast cancer

Considering the ability of miR-9 to enhance vasculogenic properties and the stronger capability of TNBC to generate vascular lacunae than luminal and HER2$^+$ carcinomas (4), we investigated whether miR-9 levels vary among the different breast cancer subtypes. In a cohort of 78 breast cancer tissues (set 1), we observed higher expression of miR-9 in TNBC than luminal and HER2$^+$ subtypes, a finding that was further validated in the TCGA public dataset (Supplementary Fig. S2A and S2B). Moreover, we observed higher miR-9 levels in tumors with high histologic grade ($P < 0.0001$) and negative hormonal status (ER $P = 0.0088$, PgR $P = 0.0007$; Supplementary Table S2). Finally, breast cancer patients were stratified according to miR-9 median expression. Kaplan–Meier survival analysis showed that higher miR-9 levels significantly associated with poor prognosis in terms of both disease-free survival (DFS) and distant-metastasis free survival (DMFS; $P = 0.0077$ and $P = 0.0121$, respectively; Supplementary Fig. S2C).

miR-9 regulates TNBC vasculogenic properties through STARD13 targeting

To identify additional miR-9 targets that might be able to explain its effect on the vasculogenic properties of TNBC, we took advantage of deposited gene profiling data of Italian and Chinese breast cancer patients (15). Tumors were stratified as luminal, $HER2^{+}$, basal, or normal-like subtype, according to intrinsic gene expression (19). Considering the overlapping expression profiles of basal and TNBC subtypes (6), we analyzed 13 basal versus 80 luminal tumors belonging to the Italian cohort of the dataset. After validating higher miR-9 expression in the basal subtype (Fig. 1D), we merged genes downregulated in basal versus luminal breast cancers with miR-9 targets predicted by at least 3 of 6 prediction tools. One of the most differentially expressed genes in our dataset, STARD13 (StAR-related lipid transfer domain containing 13 - a Rho-GAPase–activating protein), met these criteria (Supplementary Table S3). Given that downregulation of this gene has been associated with increased motility and invasion (20), we examined STARD13 as a putative mediator of miR-9 effect on TNBC vasculogenesis.

We first validated STARD13 as miR-9 target by assessing changes in the relative expression of this protein following miR-9 transfection. Consistent with STARD13 being a downstream target of miR-9 activity, we observed a slight reduction in both TNBC cell lines following this transfection (Fig. 1E). Furthermore, siRNA-mediated knockdown of STARD13 accelerated the formation of vascular-like structures, phenocopying the effects resulting from overexpression of miR-9 (Fig. 1F). Finally, miR-9–mediated suppression of luciferase activity in HEK293 cells cotransfected with a reporter fused to the 3′ UTR of STARD13 (pmiR-3′UTRWT) was abrogated by mutating at least one of the two miR-9–binding sites (Fig. 1G).

In conclusion, we show that STARD13 is directly targeted by miR-9, and this targeting comprises one of the mechanisms exploited by the miRNA to modulate the vasculogenic properties of TNBC cells.

miR-200 family inhibits tube formation ability through PDGFRβ repression

We next evaluated the basal levels of miR-200 in the same panel of TNBC cell lines, using miR-200b and miR-200c as representative members of each of the two clusters comprising the miR-200 family. We found that both miRNAs were strongly downregulated in the mesenchymal and stem-like Basal B compared with the more epithelial Basal A subgroup (Supplementary Fig. S3A). In the selected MDA-MB-231 and MDA-MB-157 cell lines, ectopic expression of both miR-200 members not only strongly impaired tube formation ability (Fig. 2A and Supplementary Fig. S3B), but also restored E-cadherin expression and, more interestingly, led to an important reduction in PDGFRβ protein levels (Fig. 2B).

As PDGFRβ is not a predicted target of miR-200, we investigated how this family could regulate the expression of the receptor. The induction of E-cadherin after miR-200 restoration is a hallmark of the suppression of ZEB1, which is a known target of miR-200 (21). This observation, combined with the possible role of ZEB1/PDGFRβ cross-talk in the maintenance of a post-EMT phenotype

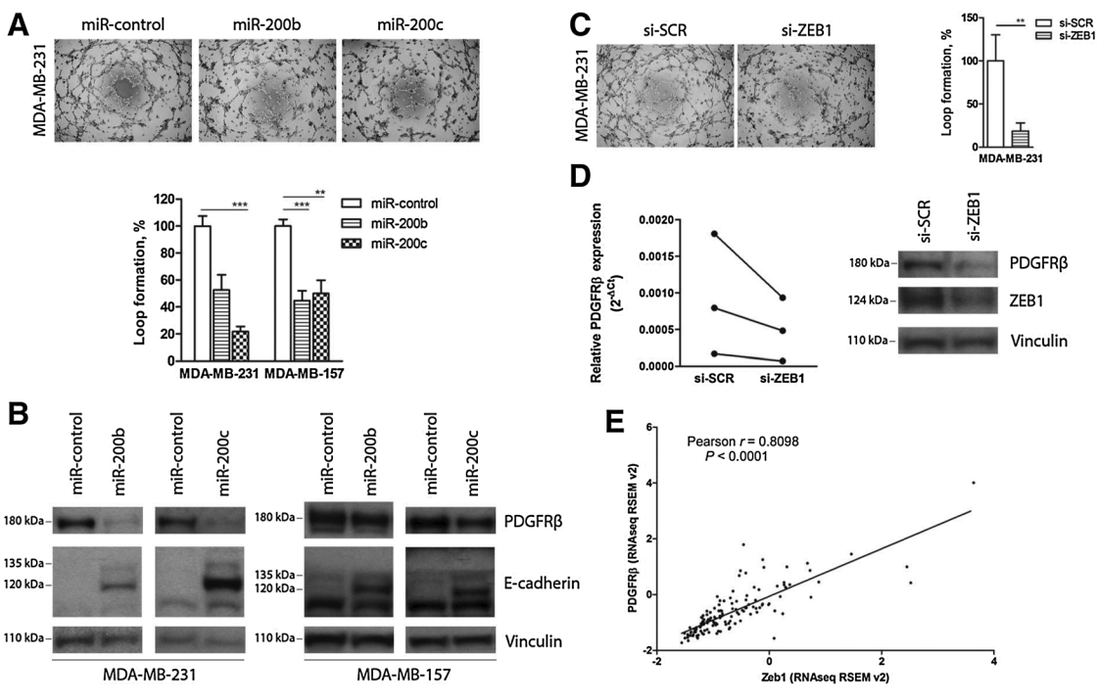

Figure 2.

miR-200 family inhibits tube formation ability through the suppression of PDGFRβ. **A** and **B,** TNBC cells were transfected with miR-200b, miR-200c, or control for 48 hours. **A,** tube formation ability was evaluated. **B,** PDGFRβ and E-cadherin expression was assessed by Western blot analysis. **C** and **D,** MDA-MB-231 cells were transfected with either a siRNA against ZEB1 or a scrambled oligonucleotide; after 72 hours, tube formation ability was analyzed (**C**); mRNA and protein levels of PDGFRβ were evaluated by qRT-PCR and Western blot analysis, respectively (**D**). **E,** correlation between *ZEB1* and *PDGFRβ* mRNA levels in the TNBC subset of TGCA public dataset. **, $P < 0.01$; ***, $P < 0.001$ (Student *t* test).

(13, 22), raised the hypothesis that miR-200 could indirectly repress PDGFRβ through ZEB1 targeting. For this reason, we first investigated the role of ZEB1 in *in vitro* loop formation. As expected, knockdown of ZEB1 reduced the ability of MDA-MB-231 cells to form vascular-like channels (Fig. 2C). Moreover, ZEB1 silencing significantly reduced PDGFRβ at both the mRNA and protein level in both MDA-MB-231 and MDA-MB-157 cell lines (Fig. 2D and Supplementary Fig. S3C–S3E). Finally, we found a strong positive correlation between mRNA levels of *ZEB1* and *PDGFRβ* in the TNBC subset of the TCGA dataset ($P < 0.001$, $r = 0.8098$; Fig. 2E).

We concluded that members of the miR-200 family inhibit the tube formation ability of TNBC cell lines through the suppression of PDGFRβ. Furthermore, the regulation of the receptor by miR-200 strongly relies on the targeting of ZEB1.

miR-9 and miR-200c regulate vascular lacunae formation *in vivo*

To validate the effect of the miRNAs of interest on vasculogenic properties *in vivo*, we first generated MDA-MB-231 clones for the stable inhibition of miR-9 (sponge miR-9) or overexpression of miR-200 (miR-200c) and the corresponding controls (sponge miR-control and vec-miR, respectively), selecting miR-200c as representative member of the family (Fig. 3A). The expanded clonal populations were implanted in the mammary fat pad of female SCID mice and monitored

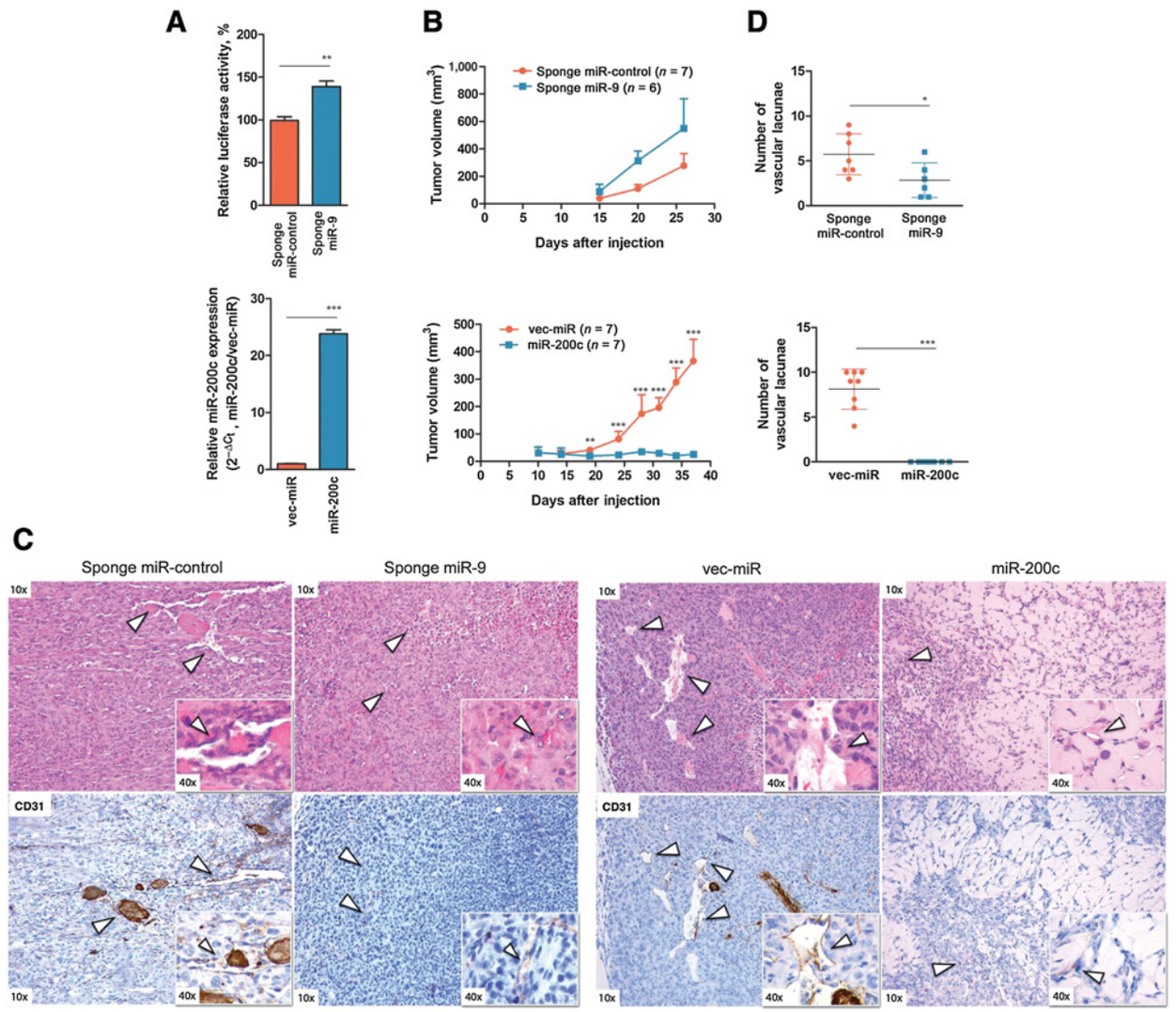

Figure 3.

miR-9 inhibition and miR-200c restoration decrease vasculogenic properties of TNBC tumors. MDA-MB-231 clones (sponge-miR-9 or miR-200c and corresponding controls) were implanted in the mammary fat pad of the SCID mice. **A,** efficiency of miR-9 inhibition and miR-200c overexpression was validated by reporter assay and qRT-PCR, respectively. For reporter assay, Firefly luciferase was normalized on *Renilla* luciferase and the luminescence activity expressed as relative value between sponge miR-9 and sponge miR-control. **B,** tumor growth was monitored by caliper measurement. **C,** hematoxylin and eosin and CD31 staining of FFPE tumor sections. White arrows indicate tumor cells engaged in vascular lacunae. **D,** quantification of vascular lacunae was performed by counting the total number of CD31$^+$ vascular structures identified in five nonoverlapping high-power microscopic fields (×400). *, $P < 0.05$; **, $P < 0.01$; ***, $P < 0.001$ (Student *t* test).

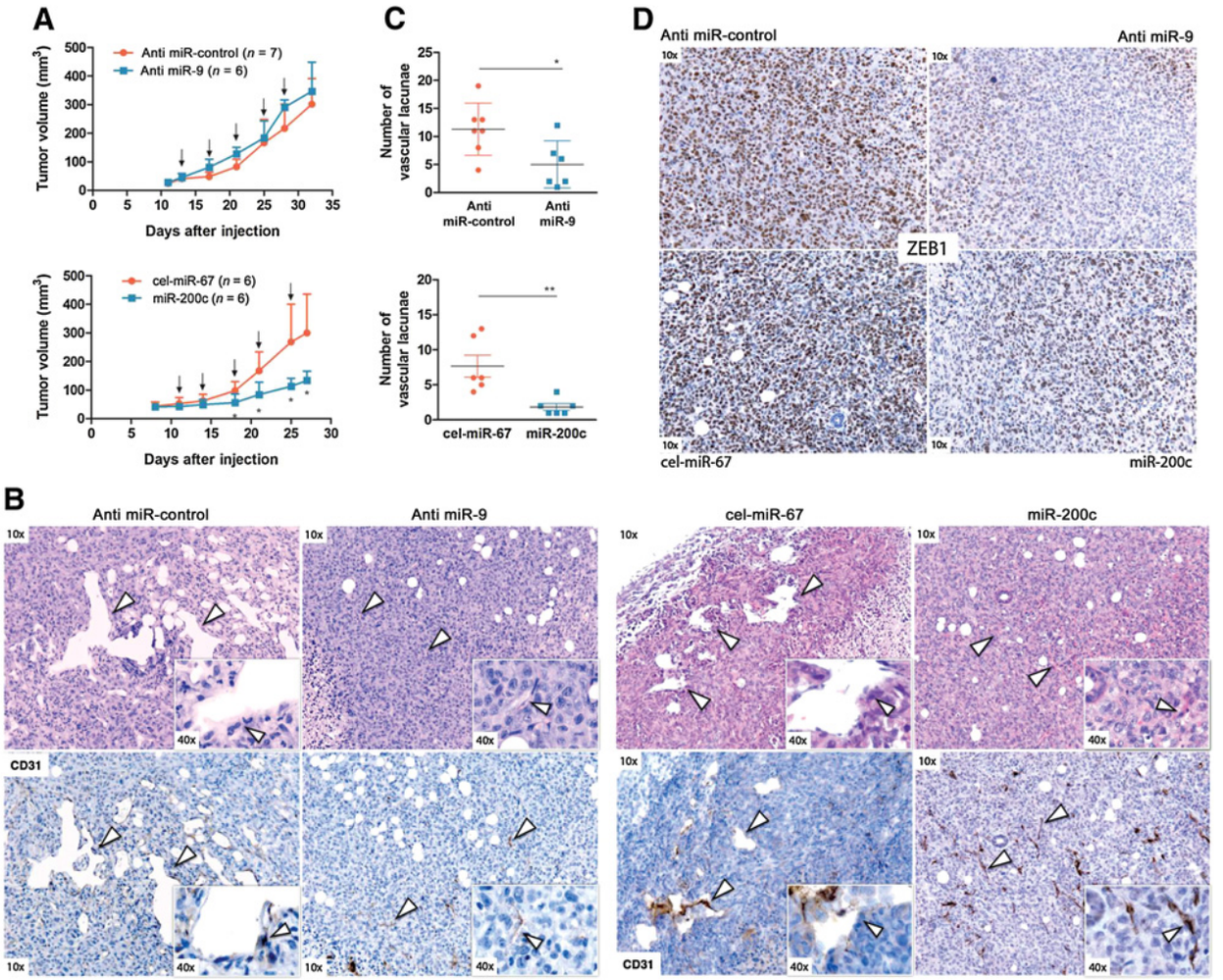

Figure 4.

In vivo treatment with miR-9 inhibitor or miR-200c mimic decreases vasculogenic properties on TNBC. MDA-MB-231 cells were implanted in the mammary fat pad of SCID mice. **A,** tumor growth was monitored; black arrows indicate the schedule of treatment. **B,** hematoxylin and eosin and CD31 staining of FFPE tumor sections. White arrows indicate tumor cells engaged in vascular lacunae. **C,** quantification of vascular lacunae was performed as described above. **D,** ZEB1 staining of FFPE tumor sections. *, $P < 0.05$; **, $P < 0.01$ (Student *t* test).

until the time of sacrifice. miR-9 knockdown did not lead to significant differences in tumor volume, whereas miR-200c tumor-bearing mice exhibited a strong reduction in tumor growth compared with control group (Fig. 3B). To assess the effect on vasculogenic properties, tumors were analyzed for the presence of vascular lacunae, identified as $CD31^+$ blood vessels with $CD31^+$ tumor cells lining the vascular structure. Qualitative analysis first revealed the presence of less structured vascular lacunae following both inhibition of miR-9 and overexpression of miR-200c in comparison with control groups (Fig. 3C). In addition, we observed a significant reduction in the number of $CD31^+$ vascular lacunae compared with the corresponding controls (Fig. 3D).

We then adopted the MDA-MB-231 cell line to perform *in vivo* miRNA delivery experiments on tumors orthotopically xenografted in SCID mice. miR-9 inhibitor or miR-200c mimic, and respective controls, were delivered by peritumoral injection. Consistently with the results obtained with stable clones, mice treated with miR-200c mimic but not those treated with miR-9 inhibitor showed a significant reduction of tumor volume (Fig. 4A). Moreover, the analysis of $CD31^+$ vascular lacunae highlighted a significant qualitative and quantitative reduction of the vasculogenic capability in treated versus untreated xenografts (Fig. 4B and C). Finally, to verify the efficiency of the delivery, histologic sections were analyzed for the expression of the EMT-associated transcription factor ZEB1. Examination of these sections revealed an overall decrease in treated samples in comparison with controls (Fig. 4D).

PDGFRβ identifies vascular lacunae in TNBC tissues

Having assessed the functional role of PDGFRβ in mediating vasculogenic properties, we evaluated the ability of the receptor to identify vascular lacunae in TNBC human tissues, as previously reported for the CD31 marker (4).

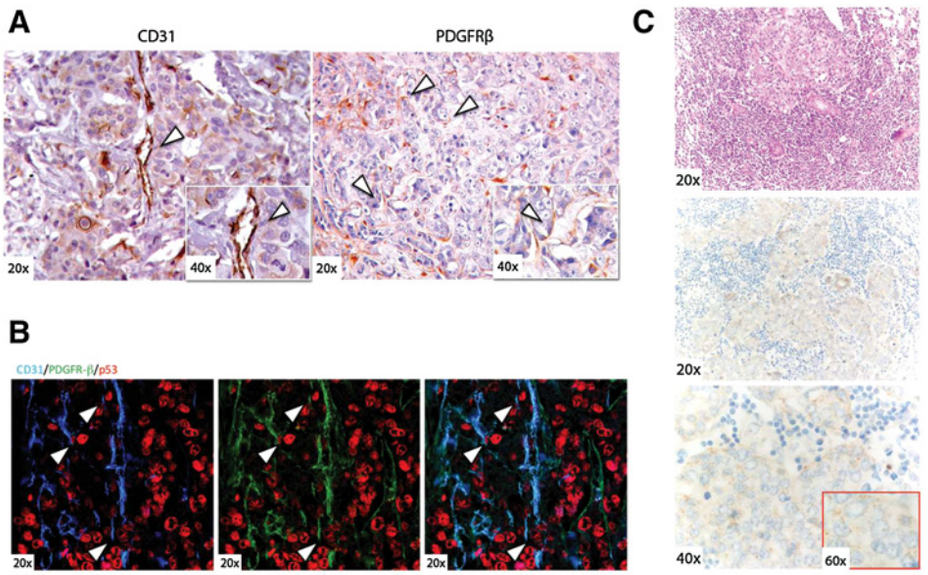

Figure 5.
PDGFRβ identifies vascular lacunae in TNBC tissues. **A,** IHC staining revealed tumor cells with reactivity for either CD31 or PDGFRβ, which participate in the formation of vascular structures (white arrows). **B,** immunofluorescence analysis of p53 (red), CD31 (blue), and PDGFRβ (green). **C,** hematoxylin and eosin staining and ISH of miR-200c. The ISH signal appeared as brown dots usually localized in the cytoplasm.

In the TNBC cohort (set 2), immunohistochemical analysis revealed a variable membrane and cytoplasmic staining of PDGFRβ in both stromal and epithelial structures. As expected, perivascular fibroblasts and pericytes associated with blood vessels were PDGFRβ positive; intratumoral stromal axes surrounding nests of neoplastic cells showed a moderate-to-intense positivity for the receptor. Finally, neoplastic cells showed a variable reactivity, ranging from absence of signal to a strong cytoplasmic and membrane staining (Supplementary Fig. S4A and S4B). More importantly, as shown for CD31 marker, also PDGFRβ was able to identify tumor cells physically engaged in the formation of vascular lacunae (Fig. 5A). To strengthen this evidence, we performed a triple-marker immunofluorescence analysis, observing foci of colocalization of PDGFRβ and CD31 in tumor cells, identified by positive reactivity to p53 staining (Fig. 5B).

TNBC tumors were then divided according to the presence ($PDGFR\beta^+$) or absence ($PDGFR\beta^-$) of PDGFRβ staining associated to tumor cells either engaged in vascular-like structures or organized in tumor nests (Table 1). We first found a strong association between the presence of $CD31^+$ and $PDGFR\beta^+$ vascular lacunae ($P = 0.001$). In addition, the presence of $PDGFR\beta^+$ vascular lacunae strongly associated also with the presence of $PDGFR\beta^+$ tumor nests ($P < 0.001$). As a consequence, 79.3% of tumors with $PDGFR\beta^+$ tumor nests showed $CD31^+$ vascular lacunae (Table 1). Interestingly, PDGFRβ expression in both tumor nests and vascular lacunae associated with high histologic grade ($P = 0.0046$; $P = 0.095$). We did not observe any significant association with other clinicopathologic parameters (Table 1).

In light of the opposite behavior of miR-9 and miR-200 family in regulating PDGFRβ-mediated vasculogenic properties, we finally evaluated the association between the expression levels of these miRNAs and the receptor status in the TNBC cohort. We found that high miR-200c levels negatively associated with the presence of $PDGFR\beta^+$ vascular lacunae ($P = 0.0444$) and established a trend of negative association with $PDGFR\beta^+$ tumor nests (Supplementary Table S4).

Finally, we qualitatively assessed the tumor distribution of miR-9 and miR-200c in TNBC by ISH. Interestingly, miR-200c expression was mainly detected in tumor cells, whereas absence of signal was observed in the stromal compartment and immune infiltrate (Fig. 5C). Conversely, we were not able to detect miR-9, probably because miR-9 expression was below the ISH detection threshold. miR-21 and scrambled miR were used as positive and as negative controls, respectively (Supplementary Fig. S4C).

Table 1. Relation between PDGFRβ expression and clinicopathologic features in TNBC human tissues

	$PDGFR\beta^+$ vascular lacunae			$PDGFR\beta^+$ tumor nest		
Clinicopathologic features	**Absence (%)**	**Presence (%)**	***P***	**Absence (%)**	**Presence (%)**	***P***
Histologic grade						
Grade II	10/45 (22.2)	0/26 (0)	0.0095	10/42 (23.8)	0/29 (0)	**0.0046**
Tumor size						
≥ T2	14/46 (30.4)	11/26 (42.3)	0.3094	15/43 (34.9)	10/29 (34.5)	0.9720
Nodal status						
Positive	16/39 (41)	12/24 (50)	0.4863	15/36 (41.7)	13/27 (48.1)	0.6084
$CD31^+$ vascular lacunae						
Presence	23/44 (52.7)	25/26 (96.1)	**0.001**	25/41(61)	23/29 (79.3)	0.1036
$PDGFR\beta^+$ tumor nest						
Presence	6/46 (13)	23/26 (88.5)	<**0.001**			

NOTE: *P* values were calculated by χ^2 test. Statistically significant values are in bold.

Discussion

Our findings indicate that miR-9 and miR-200 play opposite roles in regards to PDGFRβ-mediated vasculogenic properties of TNBC. Furthermore, we demonstrate that PDGFRβ staining identifies tumor cells physically engaged in the formation of vascular lacunae.

miR-9 has a well-recognized prometastatic function in human breast cancer (10, 23), and it has been more recently associated with poor prognosis, EMT, and stemness features (11). Consistently, we found that higher miR-9 expression identified breast cancer patients with poor prognosis and associated with high histologic grade. Moreover, miR-9 levels were higher in TNBC than in luminal and $HER2^+$ subtypes, in accordance with the negative association with hormonal status; ER can in fact mediate the epigenetic silencing of miR-9 (24), strengthening the preferential expression of this miRNA in more aggressive phenotypes.

The protumoral effects of miR-9 (e.g., migration, invasion, EMT) resemble the features mediated by PDGFRβ (25, 26). We showed indeed that miR-9 itself was able to enhance vasculogenic properties both *in vitro* and *in vivo*, resembling the addiction of TNBC to PDGFRβ signaling for the generation of vascular lacunae (4). Moreover, miR-9 expression was induced upon PDGFRβ activation, suggesting that this miRNA acts as downstream effector of the receptor signaling. Indeed, PDGF-BB–mediated induction of tube formation capability was abrogated by concomitant inhibition of miR-9, thus demonstrating that this miRNA is indeed crucial for PDGFRβ-mediated enhancement of vasculogenesis.

We identified STARD13 as a new miR-9 direct target. Despite the improvement of vasculogenic properties of TNBC cell lines after STARD13 silencing, we only partially phenocopied the effect of miR-9 overexpression. Nevertheless, it is known that miRNAs explicate their action through the targeting of multiple gene products; thus, we would need a more extensive study on miR-9 targets to fully recapitulate its effect on vasculogenesis.

Even though our data support the connection between miR-9 and PDGFRβ, in the TNBC set, we did not observe a significant association between miR-9 expression and the presence of either vascular lacunae or tumor nests positive for the receptor. However, unlike miR-200c, we were not able to reliably assess miR-9 distribution within the tumor microenvironment by ISH. As we cannot exclude other nontumoral sources of this miRNA, miR-9 levels detected by qRT-PCR might not mirror the expression in tumor cells.

The miR-200 family regulates fundamental steps of breast cancer progression, although its role in tumorigenesis still appears contradictory. This miRNA family, in fact, inhibits tumor proliferation, migration, invasion, stemness, and contributes to overcome resistance to standard therapies (21, 27–31), but its expression has been associated with breast cancer aggressiveness (32, 33). Moreover, miR-200 can either increase or reduce the metastatic potential in different TNBC models (34, 35). However, miR-200 expression is very heterogeneous within TNBC and epigenetically suppressed in undifferentiated and plastic phenotypes (36, 37). We confirmed that cell lines with mesenchymal and stem-like features (Basal B) exhibited a more significant loss in the expression of miR-200 than cells with epithelial features (Basal A); in addition, *in vivo* restoration of miR-200c in Basal B models strongly inhibited tumor growth, corroborating its tumor suppressor role. More interestingly, we described a new antitumor activity of this family consisting in the impairment of tumor cell–mediated vascularization, which is exerted through the suppression of PDGFRβ. Furthermore, the negative association between miR-200c expression and PDGFRβ-positive vascular lacunae supported the existence of this anticorrelation also in human TNBC. Finally, the predominant expression of miR-200c in tumor cells focused the miR-200/PDGFRβ cross-talk in the tumor compartment.

PDGFRβ is not, however, predicted as direct target of miR-200. Our data strongly suggest that ZEB1, one of the main transcriptional factors triggering EMT, is the link between miR-200 and PDGFRβ. Consistently, a higher PDGFRβ expression has been reported in breast cancers with a more prominent mesenchymal phenotype (38).

In vivo experiments support the effect of miR-9 knockdown and miR-200 restoration in the impairment of vascular lacunae formation. The approach of miRNA-based drug delivery raised two interesting considerations. First, miRNA treatments induced ZEB1 suppression in xenograft tumors, highlighting the ability of miR-9 and miR-200 to regulate not only tumor-mediated vasculogenesis but also, more generally, EMT. Interestingly, Twist1, another key transcriptional factor that triggers EMT, was recently reported to induce the endothelial transition of tumor cells (39). Moreover, this approach represents a proof of concept for exploiting miR-9 and miR-200 as therapeutic tools to affect tumor vascularization. The existence of pathways that act as alternatives to the canonical process of sprouting angiogenesis are proposed to mediate resistance to conventional antiangiogenic therapies (40). Intriguingly, miR-9 and miR-200 can directly induce or inhibit, respectively, also the canonical angiogenesis (41, 42), supporting their modulation as a new approach to simultaneously target different aspects of tumor vascularization.

Finally, our analyses show that PDGFRβ-expressing tumor cells identify vascular lacunae in human TNBC. More interestingly, the only detection of tumor nests positive for PDGFRβ strongly indicate the presence of vascular lacunae, suggesting that the IHC evaluation of the receptor could be useful in the identification of patients whose tumor displays this aggressive phenotype. However, the absence of PDGFRβ signal does not exclude the presence of tumor-mediated vascularization, as highlighted by the existence of $PDGFR\beta^-/CD31^+$ vascular lacunae.

In conclusion, we describe a new role of miR-9 and miR-200 in the biology of TNBC. The tight relation between PDGFRβ-miR-9 axis and EMT, with concomitant downregulation of miR-200, generates a favorable environment for the sustenance of tumor-mediated vasculogenesis, which can be impaired by treatments with miR-9 inhibitors or miR-200 mimics (Fig. 6). A deeper

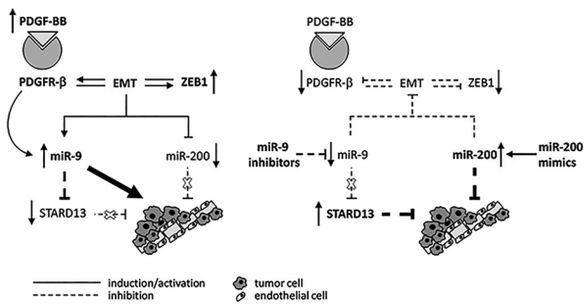

Figure 6.
Schematic representation of the network involving PDGFRβ, miR-9, miR-200, and EMT.

investigation of miR-9 and miR-200 in these multiple canonical and noncanonical pathways of vasculogenesis becomes indeed fundamental.

Disclosure of Potential Conflicts of Interest

No potential conflicts of interest were disclosed.

Authors' Contributions

Conception and design: E. D'Ippolito, I. Plantamura, F. de Braud, M.V. Iorio
Development of methodology: E. D'Ippolito, I. Plantamura, S. Baroni, C. Piovan, A.V. Gualeni, A. Gloghini, F. de Braud
Acquisition of data (provided animals, acquired and managed patients, provided facilities, etc.): L. Bongiovanni, A.V. Gualeni, A. Rossini, S. Cresta, A. Tessari, C. Tripodo
Analysis and interpretation of data (e.g., statistical analysis, biostatistics, computational analysis): E. D'Ippolito, I. Plantamura, L. Bongiovanni, P. Casalini, R. Orlandi, A. Gloghini, C. Tripodo, M.V. Iorio
Writing, review, and/or revision of the manuscript: E. D'Ippolito, I. Plantamura, L. Bongiovanni, A.V. Gualeni, A. Gloghini, S. Cresta, G. Di Leva, C. Tripodo, M.V. Iorio
Administrative, technical, or material support (i.e., reporting or organizing data, constructing databases): L. Bongiovanni
Study supervision: M.V. Iorio

Acknowledgments

Thanks to Dr. Elda Tagliabue for the useful scientific discussion; Dr. Sandra Romero-Cordoba for *in silico* analysis on public TCGA dataset; Dr. Manuela Campiglio for providing clinical–pathologic information on TNBC dataset; Dr. Cristina Ghirelli for help with cell culture; Dr. Joel Neilson for manuscript revision and critical discussion of the results; and Laura Mameli for reference editing.

Grant Support

This work was supported by a START UP AIRC grant (N 11699 to M.V. Iorio) and by a Young Investigator grant from Italian Ministry of Health.

The costs of publication of this article were defrayed in part by the payment of page charges. This article must therefore be hereby marked *advertisement* in accordance with 18 U.S.C. Section 1734 solely to indicate this fact.

Received January 21, 2016; revised May 27, 2016; accepted July 6, 2016; published OnlineFirst July 11, 2016.

References

1. Cao Z, Shang B, Zhang G, Miele L, Sarkar FH, Wang Z, et al. Tumor cell-mediated neovascularization and lymphangiogenesis contrive tumor progression and cancer metastasis. Biochim Biophys Acta 2013;1836: 273–86.
2. Ricci-Vitiani L, Pallini R, Biffoni M, Todaro M, Invernici G, Cenci T, et al. Tumour vascularization via endothelial differentiation of glioblastoma stem-like cells. Nature 2010;468:824–8.
3. Soda Y, Marumoto T, Friedmann-Morvinski D, Soda M, Liu F, Michiue H, et al. Transdifferentiation of glioblastoma cells into vascular endothelial cells. Proc Natl Acad Sci U S A 2011;108:4274–80.
4. Plantamura I, Casalini P, Dugnani E, Sasso M, D'Ippolito E, Tortoreto M, et al. PDGFRβ and FGFR2 mediate endothelial cell differentiation capability of triple negative breast carcinoma cells. Mol Oncol 2014; 8:968–81.
5. Dent R, Trudeau M, Pritchard KI, Hanna WM, Kahn HK, Sawka CA, et al. Triple-negative breast cancer: clinical features and patterns of recurrence. Clin Cancer Res 2007;13:4429–34.
6. Carey L, Winer E, Viale G, Cameron D, Gianni L. Triple-negative breast cancer: disease entity or title of convenience? Nat Rev Clin Oncol 2010; 7:683–92.
7. Criscitiello C, Gelao L, Viale G, Esposito A, Curigliano G. Investigational platelet-derived growth factor receptor kinase inhibitors in breast cancer therapy. Expert Opin Investig Drugs 2014;23:599–610.
8. Iorio MV, Croce CM. MicroRNA dysregulation in cancer: diagnostics, monitoring and therapeutics. A comprehensive review. EMBO Mol Med 2012;4:143–59.
9. Zhang J, Chintalgattu V, Shih T, Ai D, Xia Y, Khakoo AY. MicroRNA-9 is an activation-induced regulator of PDGFR-beta expression in cardiomyocytes. J Mol Cell Cardiol 2011;51:337–46.
10. Ma L, Young J, Prabhala H, Pan E, Mestdagh P, Muth D, et al. miR-9, a MYC/MYCN-activated microRNA, regulates E-cadherin and cancer metastasis. Nat Cell Biol 2010;12:247–56.
11. Gwak JM, Kim HJ, Kim EJ, Chung YR, Yun S, Seo AN, et al. MicroRNA-9 is associated with epithelial-mesenchymal transition, breast cancer stem cell phenotype, and tumor progression in breast cancer. Breast Cancer Res Treat 2014;147:39–49.
12. Hill L, Browne G, Tulchinsky E. ZEB/miR-200 feedback loop: at the crossroads of signal transduction in cancer. Int J Cancer 2013;132:745–54.
13. Meng F, Speyer CL, Zhang B, Zhao Y, Chen W, Gorski DH, et al. PDGFRalpha and beta play critical roles in mediating Foxq1-driven breast cancer stemness and chemoresistance. Cancer Res 2015;75:584–93.
14. Kong D, Li Y, Wang Z, Banerjee S, Ahmad A, Kim HR, et al. miR-200 regulates PDGF-D-mediated epithelial-mesenchymal transition, adhesion, and invasion of prostate cancer cells. Stem Cells 2009;27:1712–21.
15. Huang X, Dugo M, Callari M, Sandri M, De CL, Valeri B, et al. Molecular portrait of breast cancer in China reveals comprehensive transcriptomic likeness to Caucasian breast cancer and low prevalence of luminal A subtype. Cancer Med 2015;4:1016–30.
16. Smyth GK.Linear models and empirical bayes methods for assessing differential expression in microarray experiments. Stat Appl Genet Mol Biol 2004;3:Article3.
17. Vlachos IS, Hatzigeorgiou AG. Online resources for miRNA analysis. Clin Biochem 2013;46:879–900.
18. Gualeni AV, Volpi CC, Carbone A, Gloghini A. A novel semi-automated in situ hybridisation protocol for microRNA detection in paraffin embedded tissue sections. J Clin Pathol 2015;68:661–4.
19. Perou CM, Sorlie T, Eisen MB, van de Rijn M, Jeffrey SS, Rees CA, et al. Molecular portraits of human breast tumours. Nature 2000;406:747–52.
20. Tang F, Zhang R, He Y, Zou M, Guo L, Xi T. MicroRNA-125b induces metastasis by targeting STARD13 in MCF-7 and MDA-MB-231 breast cancer cells. PLoS ONE 2012;7:e35435.
21. Burk U, Schubert J, Wellner U, Schmalhofer O, Vincan E, Spaderna S, et al. A reciprocal repression between ZEB1 and members of the miR-200 family promotes EMT and invasion in cancer cells. EMBO Rep 2008;9:582–9.
22. Thomson S, Petti F, Sujka-Kwok I, Mercado P, Bean J, Monaghan M, et al. A systems view of epithelial-mesenchymal transition signaling states. Clin Exp Metastasis 2011;28:137–55.
23. Gravgaard KH, Lyng MB, Laenkholm AV, Sokilde R, Nielsen BS, Litman T, et al. The miRNA-200 family and miRNA-9 exhibit differential expression in primary versus corresponding metastatic tissue in breast cancer. Breast Cancer Res Treat 2012;134:207–17.
24. Hsu PY, Deatherage DE, Rodriguez BA, Liyanarachchi S, Weng YI, Zuo T, et al. Xenoestrogen-induced epigenetic repression of microRNA-9–3 in breast epithelial cells. Cancer Res 2009;69:5936–45.
25. Jechlinger M, Sommer A, Moriggl R, Seither P, Kraut N, Capodiecci P, et al. Autocrine PDGFR signaling promotes mammary cancer metastasis. J Clin Invest 2006;116:1561–70.
26. Kuzmanov A, Hopfer U, Marti P, Meyer-Schaller N, Yilmaz M, Christofori G. LIM-homeobox gene 2 promotes tumor growth and metastasis by inducing autocrine and paracrine PDGF-B signaling. Mol Oncol 2014; 8:401–16.
27. Jurmeister S, Baumann M, Balwierz A, Keklikoglou I, Ward A, Uhlmann S, et al. MicroRNA-200c represses migration and invasion of breast cancer cells by targeting actin-regulatory proteins FHOD1 and PPM1F. Mol Cell Biol 2012;32:633–51.
28. Lim YY, Wright JA, Attema JL, Gregory PA, Bert AG, Smith E, et al. Epigenetic modulation of the miR-200 family is associated with transition to a breast cancer stem-cell-like state. J Cell Sci 2013;126:2256–66.

29. Kopp F, Oak PS, Wagner E, Roidl A. miR-200c sensitizes breast cancer cells to doxorubicin treatment by decreasing TrkB and Bmi1 expression. PLoS ONE 2012;7:e50469.
30. Lin J, Liu C, Gao F, Mitchel RE, Zhao L, Yang Y, et al. miR-200c enhances radiosensitivity of human breast cancer cells. J Cell Biochem 2013; 114:606–15.
31. Bai WD, Ye XM, Zhang MY, Zhu HY, Xi WJ, Huang X, et al. MiR-200c suppresses TGF-beta signaling and counteracts trastuzumab resistance and metastasis by targeting ZNF217 and ZEB1 in breast cancer. Int J Cancer 2014;135:1356–68.
32. Madhavan D, Zucknick M, Wallwiener M, Cuk K, Modugno C, Scharpff M, et al. Circulating miRNAs as surrogate markers for circulating tumor cells and prognostic markers in metastatic breast cancer. Clin Cancer Res 2012;18:5972–82.
33. Wang J, Zhao H, Tang D, Wu J, Yao G, Zhang Q. Overexpressions of microRNA-9 and microRNA-200c in human breast cancers are associated with lymph node metastasis. Cancer Biother Radiopharm 2013;28:283–8.
34. Le MT, Hamar P, Guo C, Basar E, Perdigao-Henriques R, Balaj L, et al. miR-200-containing extracellular vesicles promote breast cancer cell metastasis. J Clin Invest 2014;124:5109–28.
35. Knezevic J, Pfefferle AD, Petrovic I, Greene SB, Perou CM, Rosen JM. Expression of miR-200c in claudin-low breast cancer alters stem cell functionality, enhances chemosensitivity and reduces metastatic potential. Oncogene 2015;34:5997–6006.
36. Castilla MA, Diaz-Martin J, Sarrio D, Romero-Perez L, Lopez-Garcia MA, Vieites B, et al. MicroRNA-200 family modulation in distinct breast cancer phenotypes. PLoS ONE 2012;7:e47709.
37. Riaz M, van Jaarsveld MT, Hollestelle A, Prager-van der Smissen WJ, Heine AA, Boersma AW, et al. miRNA expression profiling of 51 human breast cancer cell lines reveals subtype and driver mutation-specific miRNAs. Breast Cancer Res 2013;15:R33.
38. Ahmad A, Wang Z, Kong D, Ali R, Ali S, Banerjee S, et al. Platelet-derived growth factor-D contributes to aggressiveness of breast cancer cells by up-regulating Notch and NF-kappaB signaling pathways. Breast Cancer Res Treat 2011;126:15–25.
39. Chen HF, Huang CH, Liu CJ, Hung JJ, Hsu CC, Teng SC, et al. Twist1 induces endothelial differentiation of tumour cells through the Jagged1-KLF4 axis. Nat Commun 2014;5:4697.
40. Vasudev NS, Reynolds AR. Anti-angiogenic therapy for cancer: current progress, unresolved questions and future directions. Angiogenesis 2014;17:471–94.
41. Pecot CV, Rupaimoole R, Yang D, Akbani R, Ivan C, Lu C, et al. Tumour angiogenesis regulation by the miR-200 family. Nat Commun 2013; 4:2427.
42. Zhuang G, Wu X, Jiang Z, Kasman I, Yao J, Guan Y, et al. Tumour-secreted miR-9 promotes endothelial cell migration and angiogenesis by activating the JAK-STAT pathway. EMBO J 2012; 31:3513–23.